AGU PUBLICATIONS

JGR

Journal of Geophysical Research: Atmospheres

RESEARCH ARTICLE
10.1002/2017JD027139

Special Section:
Studies of Emissions and Atmospheric Composition, Clouds and Climate Coupling by Regional Surveys, 2013 (SEAC4RS)

Key Points:
- Tropospheric ozone anomalies are anticorrelated (or correlated) with water vapor (or temperature) with a correlation coefficient about 0.6
- The regression slopes between ozone and temperature anomalies for surface, PBL, and midtroposphere are within 3.0–4.1 ppbv/K
- The stratospheric influence on free-tropospheric ozone could be significant during early summer

Supporting Information:
- Supporting Information S1

Correspondence to:
S. Kuang,
kuang@nsstc.uah.edu

Citation:
Kuang, S., Newchurch, M. J., Thompson, A. M., Stauffer, R. M., Johnson, B. J., & Wang, L. (2017). Ozone variability and anomalies observed during SENEX and SEAC^{4}RS campaigns in 2013. *Journal of Geophysical Research: Atmospheres, 122*, 11,227–11,241. https://doi.org/10.1002/2017JD027139

Received 15 MAY 2017
Accepted 6 OCT 2017
Accepted article online 12 OCT 2017
Published online 30 OCT 2017

Ozone Variability and Anomalies Observed During SENEX and SEAC^{4}RS Campaigns in 2013

Shi Kuang[1], Michael J. Newchurch[2], Anne M. Thompson[3], Ryan M. Stauffer[3,4], Bryan J. Johnson[5], and Lihua Wang[1]

[1]Earth System Science Center, University of Alabama in Huntsville, Huntsville, AL, USA, [2]Atmospheric Science Department, University of Alabama in Huntsville, Huntsville, AL, USA, [3]Earth Science Division, NASA Goddard Space Flight Center, Greenbelt, MD, USA, [4]Universities Space Research Association, Columbia, MD, USA, [5]Global Monitoring Division, NOAA Earth System Research Laboratory, Boulder, CO, USA

Abstract Tropospheric ozone variability occurs because of multiple forcing factors including surface emission of ozone precursors, stratosphere-to-troposphere transport (STT), and meteorological conditions. Analyses of ozonesonde observations made in Huntsville, AL, during the peak ozone season (May to September) in 2013 indicate that ozone in the planetary boundary layer was significantly lower than the climatological average, especially in July and August when the Southeastern United States (SEUS) experienced unusually cool and wet weather. Because of a large influence of the lower stratosphere, however, upper tropospheric ozone was mostly higher than climatology, especially from May to July. Tropospheric ozone anomalies were strongly anticorrelated (or correlated) with water vapor (or temperature) anomalies with a correlation coefficient mostly about 0.6 throughout the entire troposphere. The regression slopes between ozone and temperature anomalies for surface up to midtroposphere are within 3.0–4.1 ppbv K^{-1}. The occurrence rates of tropospheric ozone laminae due to STT are ≥50% in May and June and about 30% in July, August, and September suggesting that the stratospheric influence on free-tropospheric ozone could be significant during early summer. These STT laminae have a mean maximum ozone enhancement over the climatology of 52 ± 33% (35 ± 24 ppbv) with a mean minimum relative humidity of 2.3 ± 1.7%.

1. Introduction

In 2013, two field campaigns, the Southeast Nexus (SENEX) (Warneke et al., 2016) and the Studies of Emissions and Atmospheric Composition, Clouds and Climate Coupling by Regional Surveys (SEAC^{4}RS) (Toon et al., 2016), were conducted over the Southeastern United States (SEUS) covering a broad range of atmospheric chemistry and air quality science investigations. These campaigns are critical to improving the accuracy of emissions inventories in chemical transport models (Travis et al., 2016) and our understanding of the interaction between natural and anthropogenic emissions (e.g., isoprene-ozone chemistry (Yu et al., 2016)).

Ozone is a crucial tropospheric trace gas that drives the complex oxidization chain by reacting with carbon monoxide, methane, hydrogen oxide radicals (HO_x), nitrogen oxide radicals (NO_x), and volatile organic compounds (VOCs) (Jacob, 2000). Tropospheric ozone abundance and variability are regulated by stratosphere-to-troposphere transport (STT), industrial emissions, lightning-generated NO_x, and biomass burning (Lelieveld & Dentener, 2000). Although ozone is a secondary pollutant in the troposphere, the stratosphere, containing 90% of the total ozone burden, is a direct source. This direct natural source of ozone adds to the complexity of accurate source quantification and air quality regulation policy making (Lin et al., 2012). Based on model studies, STT is expected to maximize during winter or early spring, and to minimize in the summer for the extratropics in terms of intrusion frequency (Elbern et al., 1997) and net downward flux transport (Wernli & Bourqui, 2002). However, previous field campaigns suggest that the stratospheric source still contributes significantly to the tropospheric ozone budget in North American midlatitudes during the summertime (Bourqui & Trépanier, 2010; Bourqui et al., 2012; Škerlak et al., 2014; Stauffer et al., 2017; Tarasick et al., 2007; Thompson et al., 2015, 2007, 2008; Yorks et al., 2009). The global-scale STT budget is driven fundamentally by the large-scale stratospheric circulation (Hess & Zbinden, 2013). While STT does not often directly influence surface ozone amounts in the eastern U.S. (Ott et al., 2016), higher elevations in the intermountain western U.S. are more likely to experience direct, stratospheric influence (Langford et al., 2012; Lefohn et al., 2012, 2014; Lin et al., 2012). Coupled chemistry-climate model simulations

suggest a positive trend for the STT source as a response to enhanced stratospheric circulation and to future climate change (Neu et al., 2014; Sudo et al., 2003).

Huntsville is a near sea level (200 m above sea level (asl)), midsized city located at the southern edge of the northern middle latitudes with a humid subtropical climate, primarily characterized by hot summers and abundant, year-round precipitation. The air quality of Huntsville can be largely considered as slightly polluted rural, given that ozone in the planetary boundary layer (PBL) at Huntsville is higher than unpolluted, background stations (e.g., Trinidad Head, California; Boulder, Colorado; and Wallops Island, Virginia) (Newchurch et al., 2003; Stauffer et al., 2016), especially during the summer, but lower than polluted metropolitan cities (e.g., Houston) (Morris et al., 2010). Although industrial emissions in Huntsville are minor, this city is sometimes affected by pollution transport on various spatial scales (Kuang et al., 2011; Reid et al., 2017).

The primary objective of this work is to analyze tropospheric ozone variability and anomalies using the ozonesonde data measured during SENEX and SEAC^{4}RS in 2013. The second objective is to quantify the stratospheric influence on tropospheric ozone. Thereafter, "13-May-Sep" will be used to represent the campaign duration from May to September 2013, which encompasses the typical "ozone season" (Cox & Chu, 1996) and to cover the potential spring surface maxima (Monks, 2000) and summer tropospheric maxima (Fusco & Logan, 2003).

2. Ozonesondes

Ozonesondes are currently the most widely used instrument to measure vertical ozone profiles from the surface up to the midstratosphere due to their well-characterized behavior and working capability under various sky conditions despite their relatively long preparation and measurement time (see review article by Thompson et al., 2011). The inherent response time (e^{-1}) is typically between 20 and 30 s, which corresponds to a vertical resolution of 100–150 m given a typical balloon rise rate at approximately 5 m s^{-1}. Assessment experiments suggest that ozonesondes measure ozone with a precision better than ±5% and an accuracy better than ±10% up to about 35 km if the sondes are prepared and operated properly, although there exist systematic biases of less than 7% with different sensing solution and manufacturer years (Johnson et al., 2008, 2002; Komhyr et al., 1995; Smit et al., 2007). The Huntsville ozonesonde station (34.725°N and 86.645°W) is a joint effort between the University of Alabama in Huntsville (UAH) and NOAA's Global Monitoring Division (formerly known as the Climate Monitoring and Diagnostic Laboratory) in the Earth System Research Laboratory. Since 1999, weekly electrochemical concentration cell-type ozonesonde (model: ENSCI 2Z) observations (Komhyr, 1969) have been made at UAH to measure ozone (Newchurch et al., 2003) for various scientific research (e.g., Li et al., 2005) and satellite validation efforts (Nassar et al., 2008; Wang et al., 2011). The quick-look curtain plots of the ozonesonde data taken during SEAC^{4}RS are available at the webpage of SouthEast American Consortium for Intensive Ozonesonde Network Study (SEACIONS, http://ozone.met.psu.edu/dev/research/seacions/quicklooks.php).

The atmospheric thermodynamic and wind profiles are usually measured by an independent radiosonde located in the ozonesonde package. At the Huntsville station, all radiosondes before August 2012 (flight number $<$ 749) employed Vaisala RS80 to measure ambient temperature, pressure, and relative humidity (RH). After August 2012, most flights were made with the iMet radiosondes that added measurements of wind velocity, wind direction, and Global Position System altitude, while a few others were still made with Vaisala RS80. From May to September 2013, 43 out of 48 ozonesondes attached iMet radiosondes. RH is used to determine water vapor in this study because it is directly available from radiosonde measurements (Wang et al., 2002). The measurement uncertainties of temperature, pressure, and RH of a radiosonde vary with the factory type, model, and manufacturer batch of the radiosonde. Stauffer et al. (2014) reported that iMet measured a slightly higher atmospheric pressure than the Vaisala RS80. However, this difference has negligible impact on the ozone mixing ratio calculation below 20 km. We do not know the difference of temperature and RH measurements between RS80 and iMet. Using RS92 as a quality reference, intercomparison experiments suggest that on average, iMet temperature measurements report about 0.5°C lower than RS92 (Hurst et al., 2011) and RS80 reported about 0.1°C lower than RS92 in the troposphere during the daytime (Steinbrecht et al., 2008). In terms of RH, iMet reports about 1–2% (ΔRH) moister than RS92 below 20 km (Hurst et al., 2011), while RS80 measures 0–20% (ΔRH/RH) more moist than RS92 below 10 km (Miloshevich

et al., 2006). Thus, mixing the usage of Vaisala RS80 and iMet radiosonde data has negligible impact on our later analyses of the ozonesonde data.

3. Tropospheric Ozone Variability in 2013 Compared to Climatology

Figure 1 presents the time-height ozone and RH curtains from the ozonesonde measurements during 13-May-Sep for SENEX and SEAC^{4}RS campaigns. The launch date and time of each individual profile is provided in Table S1 in the supporting information. These data are averaged to 100 m bins to reduce random errors and for consistency with ozonesonde vertical resolution. The thermal tropopause heights are calculated with the World Meteorological Organization (WMO) (1986) definition, which is based on the temperature lapse rate. The thermal tropopause is approximately 1 km higher than the ozone tropopause (Bethan et al., 1996; Pan et al., 2004). Weekly ozonesondes were launched from May to July, while some extra daily ozonesondes were launched during August and September. Many time-discontinuous tropospheric ozone laminae appear on the daily ozonesonde profiles in Figure 1 suggesting that many of these laminae were driven by relatively short-term processes. As expected, tropopause heights generally increased from about 11 km in early May to about 15 km in July and mostly oscillated around 15 km in August and September, similar to the seasonal tropopause height variation observed in Houston in 2006 (Thompson et al., 2008).

Figure 2 compares the average ozonesonde profile of 13-May-Sep to the Huntsville climatological average of the same months. The climatology of ozone, temperature, and RH is calculated using the weekly ozonesonde data (737 profiles), mostly taken near 1800 UTC (local time 1200 or 1300) on Saturdays, from 1999 to 2012. The tropospheric ozone mixing ratio in Huntsville during 13-May-Sep generally increases with altitude similar to climatology largely because the sinks of ozone, such as water vapor and HO_x, generally decrease with altitude (Ren et al., 2008). Both the mean ozone profile of 13-May-Sep and the climatology show a positive gradient near the surface indicative of the important ozone sink of surface deposition. The 13-May-Sep ozone averages about 10 ppbv (about 17%) lower than the climatology in the PBL, is close to the climatology in the midtroposphere, and is about 40 ppbv (about 25%) higher than the climatology in the upper troposphere. The variability of the 13-May-Sep ozone in the upper troposphere is much larger than the variability of the climatology. The mean thermal tropopause height during 13-May-Sep is 14.4 km, slightly lower than the climatology of 14.7 km. However, the ozone average at the mean tropopause height for 13-May-Sep is 220 ppbv, much higher than the climatology of 180 ppbv. The enhanced ozone and large variability in the upper troposphere and lower stratosphere (UTLS) strongly suggest an exceptional influence of the lower stratosphere on the upper troposphere in 13-May-Sep.

Figure 3 shows the monthly averaged ozone and ozone variability as well as ozone, temperature, and RH anomalies for 13-May-Sep relative to the climatology. The tropopause height increase from late spring to early summer reflects its seasonal variation following the underlying tropospheric temperature variation (Seidel et al., 2001). In Figure 3a, the ozone mixing ratios in the mid-troposphere peaked in May and August ($>$70 ppbv). The August peak is a persistent feature in the Huntsville-based climatological data (Newchurch et al., 2003; Stauffer et al., 2016) and is associated with more active photochemical production in August. In addition, this August peak in Huntsville is also a geographic maximum according to Li et al. (2005) and Cooper et al. (2007) who discovered that ozone between 6 and 11 km above Huntsville during summer was measured to be 10–20 ppbv higher than other North American stations due to the persistent upper level anticyclone over the SEUS, which "traps" and "cooks" the convectively lofted ozone and ozone precursors such as lightning NO_x. The local ozone peak between 5 and 9 km in May 2013 is not a permanent feature for Huntsville and is 10–30 ppbv higher than the climatology (Figure 3b). For summer (June, July, and August) 2013, the generally negative anomalies below 9 km, especially in July, can be explained by the negative anomalies of 500 hPa geopotential height and temperature (Stauffer et al., 2016) in Huntsville as shown in Figure 4. The anomalies are calculated by considering the average between 1999 and 2012 as climatology, similar to the ozone calculation. This 500 hPa anomalous pattern is related to the unusually strong ridge in the western U.S. at this time (Toon et al., 2016). The agreement between the anomalous ozone and geopotential height suggests that free-tropospheric ozone enhancement in the SEUS is correlated to the intensity of a persistent upper anticyclone in that region as hypothesized by Li et al. (2005).

Figure 3c presents the potential vorticity (PV) anomaly at Huntsville calculated from the reanalyzed ERA-Interim global meteorological data set with 37 pressure levels, 0.7° × 0.7° spatial resolution, and 6 h

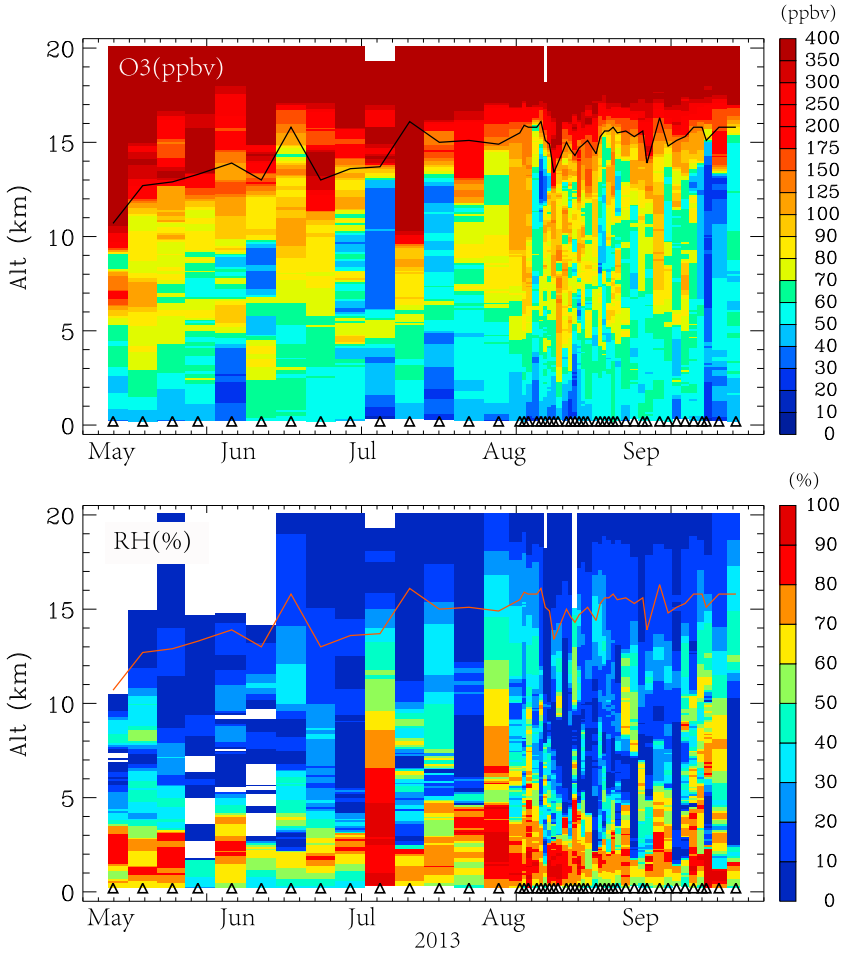

Figure 1. Time-height cross section of (top) ozone mixing ratio and (bottom) RH from ozonesonde measurements in Huntsville, AL, from May to September 2013 during SENEX and SEAC^{4}RS. The solid line represents the WMO-defined thermal tropopause (WMO, 1986), and the triangles at the bottom mark the measurement dates.

interval (Dee et al., 2011). The PV profiles closest to Huntsville and the ozonesonde measurement time are selected to calculate the PV anomaly in the same manner as for the ozonesonde data processing. Because PV is an effective tracer for stratospheric air (Danielsen, 1968), analysis of PV anomaly, especially around the tropopause, is helpful to diagnose the yearly STT variations. Both the upper troposphere and lower stratosphere show similarly positive ozone, positive PV, positive temperature, and negative RH anomalies in May, June, and July (Figures 3b–3d) suggesting that the stratospheric source played an important role for the positive ozone anomalies in the UTLS in these months (Terao et al., 2008), consistent with our earlier analysis in this paper. However, the PV anomaly is not obviously correlated with the ozone anomaly below 10 km. The large variability of ozone in the upper troposphere in July, shown in both Figures 1 and 3e, is atypical and due to either a STT or a depressed-tropopause event on 13 July 2013 (HU795) and two low-ozone days on 6 July (HU794) and 20 July (HU796) 2013. On the HU795 profile, the thermal tropopause was located at 16.1 km, but the 2 PV unit (PVU)-based dynamic tropopause was at 8.5 km. This tropopause-height identification discrepancy occurs because the thermal tropopause sometimes is unable to capture the small-scale dynamic deformation although it captures the thermal stratification well (Wirth, 2000). These two low-ozone days had some common features: cloudy and low ozone both in the PBL (20–30 ppbv) and upper troposphere (30–40 ppbv). There was rain during frontal passage on 6 July. These facts suggest that the low upper tropospheric ozone amounts on 6 and 20 July were likely primarily due to convective transport of the low-ozone air masses from the PBL. For August and September 2013, the ozone has a negative anomaly (−20%–0) (Figure 3b) from 10 km up to ~15 km, correlated with the positive RH anomaly (Figure 3d), and a positive anomaly (mostly 0–10%) from 4 to 8 km, correlated with

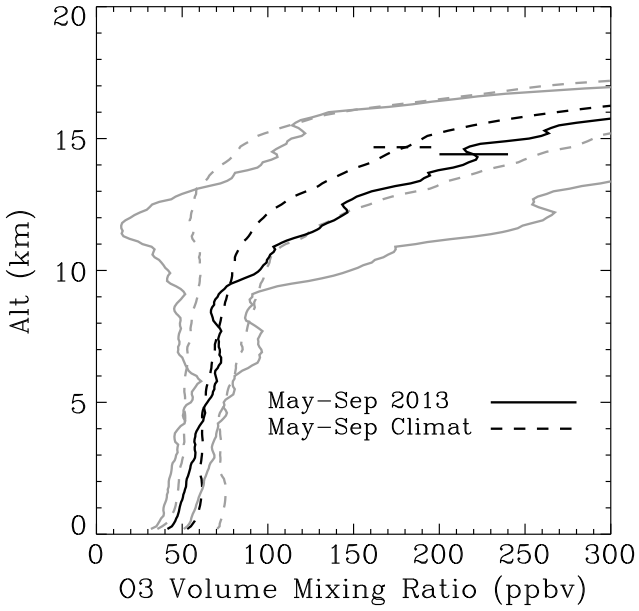

Figure 2. Comparison of the average ozonesonde profile at Huntsville from May to September 2013 (solid) to the 13 year climatology (dashed). The climatology is calculated with the weekly ozonesonde data from 1999 to 2012. The gray lines represent the 1σ standard deviations. The horizontal lines between 14 and 15 km represent the average thermal tropopause.

the positive temperature anomaly. Climatologically, the net downward cross-tropopause flux decreases from spring to summer and minimizes in September for Northern Hemisphere extratropics (Škerlak et al., 2014; Wernli & Bourqui, 2002). The ozone and RH anomaly structures at UTLS in Figures 3b and 3d suggest that the net downward cross-tropopause flux is significantly higher than the climatology for May, June, and July, whereas the net upward cross-tropopause flux (such as convection) is moderately higher than the climatology for August and September 2013 in Huntsville.

It is worth noting that the ozone and temperature anomalies in the UTLS are generally anticorrelated with the temperature in the middle and lower troposphere as shown by Figure 3d. For example, the UTLS was warm from May to July while the middle and lower troposphere was cold, relative to the climatology. This can be explained by vertical motions in the lower stratosphere, which compensated opposite vertical motions in the troposphere (Reed, 1950; Steinbrecht et al., 2003). Upward motion in a cyclonic system leads to a cold troposphere because of adiabatic cooling. The tropopause altitude sinks resulting in adiabatic warming in the lower stratosphere and vice versa.

In the PBL, the ozone anomalies correlate well with both the temperature and RH anomalies. The PBL in 13-May-Sep was relatively wet and cool with low ozone except for June during which the PBL-averaged ozone was slightly higher (~2%) than the climatology. The ozone average in the PBL during both July and August was about 40% lower than the climatology partly because of recent, consistent NO_x emission reduction (Hidy et al., 2014) and partly because of high moisture and low temperature. Transport from a cleaner marine source is not a primary cause for low PBL ozone observed in Huntsville because of two reasons. First, low PBL ozone mostly occurred during frontal passages and rain. Second, the average winds in the PBL in summer 2013 were dominated by weak westerly flow. In fact, the sonde-measured meteorological data in Huntsville accurately represented the state of the SEUS in 2013, wetter and much cooler than average (Blunden & Arndt, 2014). There is a consensus that temperature is the most important meteorological factor to affect surface ozone, especially during the summer (e.g., Cox & Chu, 1996; Vukovich & Sherwell, 2003) because temperature affects chemical reaction rates and emissions of ozone precursors. In some urban areas, a linear regression between surface temperature and ozone can even be used as a predictor for ozone (Bloomer et al., 2009; Dueñas et al., 2002; Im et al., 2011). Ozone generally has a negative correlation with RH because of the heterogeneous loss of the catalysts in the ozone production chain, which are primarily HO_x and NO_x (Jacob, 2000). In addition, RH is correlated with sky cover (e.g., cloud and wet aerosols), which significantly affects the ozone production through the radiation flux and temperature. Therefore, the temperature and RH are covarying in their effects on near-surface ozone.

4. Correlation Among Tropospheric Ozone, Water Vapor, and Temperature

Meteorological factors notably affected the chemical processes that influence ozone concentrations. Investigation of the relationship between ozone and these factors is necessary to account for meteorological effects when examining air quality trends (Lin et al., 2014; Wise & Comrie, 2005). Figure 5a presents the correlation between tropospheric ozone and RH anomalies to further quantify their relationship at different altitudes using the same monthly averaged data as in Figure 3. We specify the layer from PBL top to 9 km asl as the midtroposphere and the layer from 9 km asl to tropopause as the upper troposphere. This specification is based on the possibility of influential sources and is somewhat arbitrary. The ozone and RH anomalies are strongly anticorrelated with Pearson correlation coefficients (r) from −0.55 to −0.92 in all altitude layers within the troposphere. Their correlations are the strongest at the surface (with sufficient significance, $r = -0.92$, ρ value = 0.027). Because of the small sample size in this study, the extremely high correlation at the surface should not be overinterpreted. The ozone/RH regression

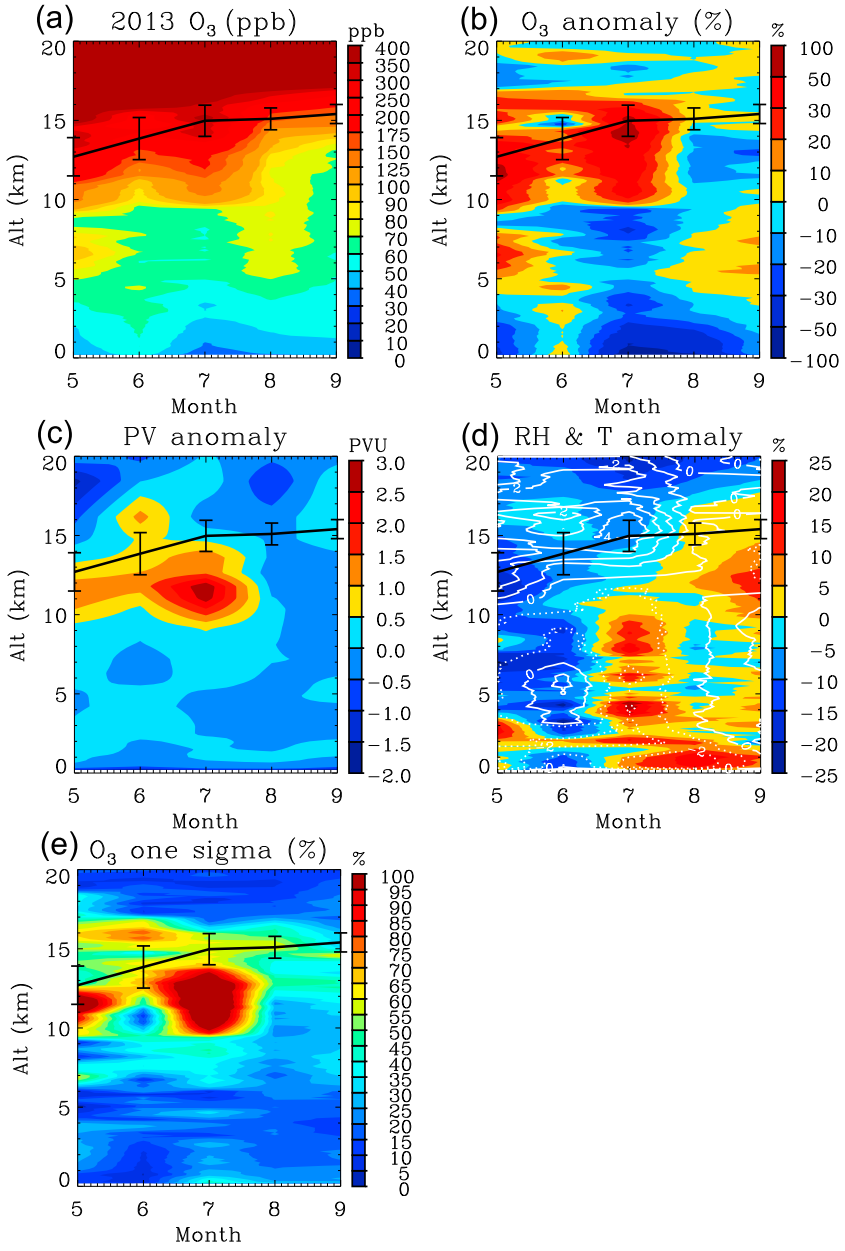

Figure 3. The 13-May-Sep ozonesonde measurements at Huntsville compared to the climatology. (a) Monthly mean ozone mixing ratio and tropopause heights with their 1σ standard deviations. (b) Ozone anomaly for 13-May-Sep. (c) PV anomaly for 13-May-Sep computed from the global ERA-Interim model (Dee et al., 2011). (d) RH anomaly (colors) and temperature anomaly (white lines). White solid lines represent positive anomaly and white dotted lines refer to negative anomaly. (e) Monthly 1σ standard deviation of ozone observed during 13-May-Sep. The black solid line represents the thermal tropopause heights and the vertical bars represent the 1σ standard deviations of the tropopause heights.

slopes are −1.0, −0.6, −0.5, and −3.6 ppb·%$^{-1}$ for the surface, PBL, midtroposphere, and upper troposphere, respectively. The regression linear slope for the upper troposphere is significantly different from the slopes at the surface, PBL, and midtroposphere (Pan et al., 2004) because the upper troposphere is affected more by the stratosphere so that the upper tropospheric ozone change with respect to water vapor change is much larger than lower altitudes (Homeyer et al., 2011). Water vapor plays different roles in the upper troposphere compared to lower layers in terms of its negative correlation with ozone. In the PBL, photolysis in the presence of water vapor (to produce OH) is the major sink for tropospheric ozone (Jacob & Winner, 2009). While in the upper troposphere, besides this chemical sink effect, the negative correlation between ozone and water vapor results from the physical

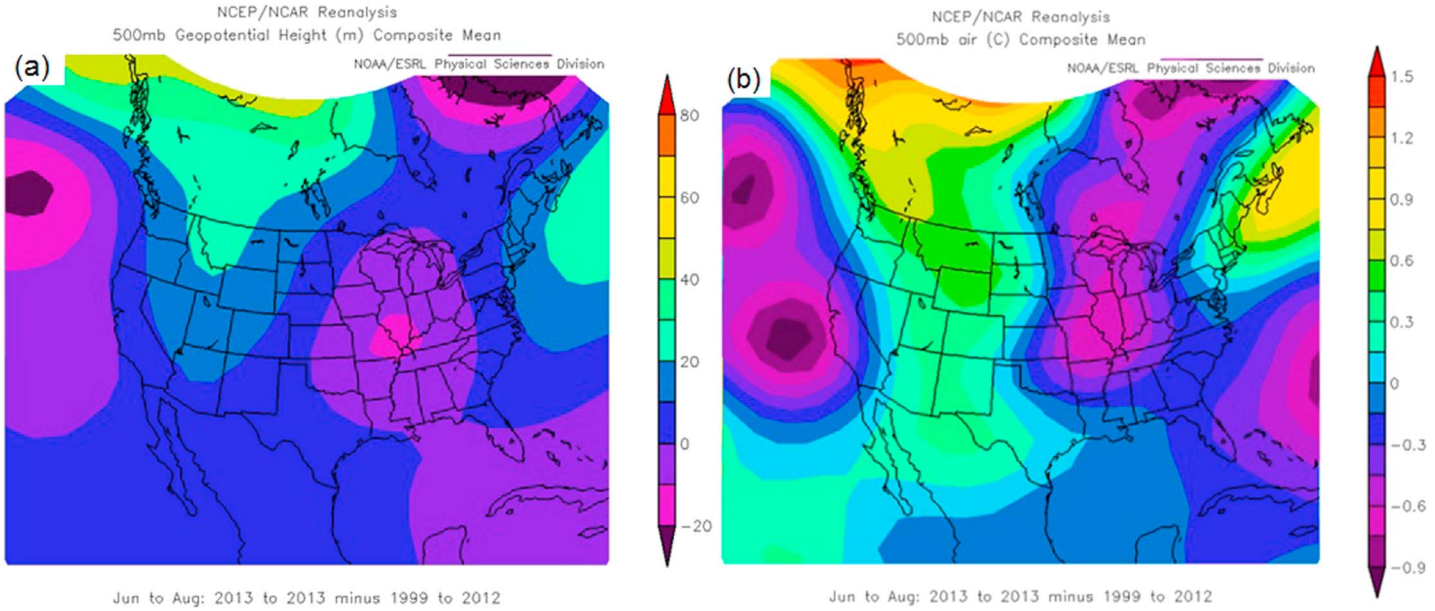

Figure 4. The 2013 summer (June, July, and August) anomaly for (a) 500 hPa geopotential height and (b) 500 hPa temperature explaining weaker-than-climatology summertime ozone observed at Huntsville (source: NOAA/ESRL, http://www.esrl.noaa.gov/).

downward mixing of dry stratospheric air. The general anticorrelation between ozone and water vapor should be seen as an accompanying linkage instead of a cause-and-effect relationship because of the complicated feedback among ozone, water vapor, and climate.

Conversely, water vapor can be seen as a proxy for convection or clouds under certain circumstances. The positive correlation between ozone and water vapor could be observed during the convective transport of ozone or its precursors from the polluted PBL (Dickerson et al., 1987), or when the lightning-generated NO_x is significant (DeCaria et al., 2005; Wang et al., 2015).

In Figure 5b, the temperature anomalies closely correlate with the ozone anomalies showing similar r values (0.63–0.71) at all layers except for the midtroposphere (r = 0.36). This means that the temperature variations can explain around 40% (r^2) of the tropospheric ozone variations outside of the midtroposphere. Higher temperature is generally favorable for ozone precursor emissions, ozone production, and air pollutant accumulation especially in a polluted region (with weaker relationships in unpolluted areas). The

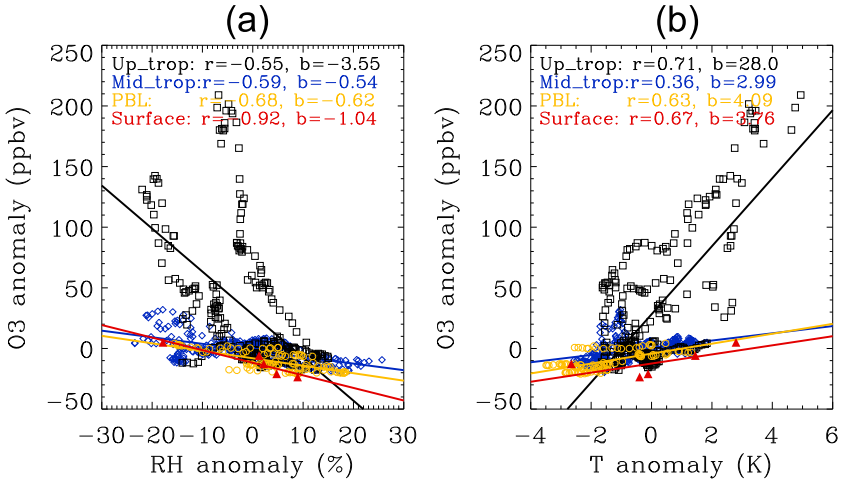

Figure 5. Correlation (a) between ozone anomaly and RH and (b) between ozone anomaly and temperature for surface (red triangle), PBL (yellow circle), midtroposphere (blue diamond), and upper troposphere (black square) calculated from the monthly averaged ozonesonde data from May to September 2013. "*r*" represents the Pearson correlation coefficient, and "*b*" represents the regression slope.

ozone/temperature linear slopes for the surface (3.8 ppbv K^{-1}) and PBL (4.1 ppbv K^{-1}) are generally consistent with previous studies in a similar region (Olszyna et al., 1997; Rasmussen et al., 2012). The linear slope for the upper troposphere (28.0 ppbv K^{-1}) is significantly distinct from the lower altitudes because of different mechanisms similar to the RH-ozone relationship discussed above. Obviously, the upper troposphere is affected more by the lower stratosphere where the ozone and temperature are typically correlated and vary together with solar cycle, quasi-biennial oscillation, and El Niño–Southern Oscillation (Logan et al., 2003; Randel & Cobb, 1994). The poor correlation between ozone and temperature anomalies in the midtroposphere results from some outliers in May corresponding to considerable positive ozone anomalies (0–35 ppbv) due to the STT influences (also see Figures 3b and 3d), but with slightly negative temperature anomalies (about −1 K). The temperature of these enhanced ozone layers is slightly lower than the climatology but may be still warmer than the background temperature at the same altitudes because of isentropic descent.

The correlation between ozone and RH (or temperature) in Figure 5 underscores the importance of careful data interpretation of ozone and its tracers. The value of the correlation coefficient (either high or low), which indicates the strength of relationship, does not necessarily attribute the cause to any emission source since the coefficients can be similar for anthropogenic and stratospheric sources. In addition, the correlation coefficients can be highly sensitive to the selection of samples. A weak correlation is expected by mixing two categories with different properties. However, the slope and intercept of the regression are often more meaningful for source attribution.

5. Stratospheric Influence on Midtropospheric and PBL Ozone

To investigate the stratospheric influence on midtropospheric and PBL ozone, we analyzed the enhanced ozone layers below 9 km due to STT for the 2013 ozone season. The upper troposphere is not included for two reasons. First, the layer identification in the upper troposphere is significantly affected by the tropopause definition and it is difficult to tell whether or not the layer below the tropopause has been irreversibly mixed into the troposphere. Second, the uncertainty of RH measurements in the upper troposphere is relatively high (Hurst et al., 2011; Miloshevich et al., 2006). The STT (stratospheric intrusion) layers are identified by four mandatory criteria plus two optional pieces of evidence. Modified from previous literature (Beekmann et al., 1997; Newell et al., 1999; Stohl et al., 2000), the four mandatory criteria are (1) maximum ozone in the identified layer is at least 25% greater than the reference ozone, (2) minimum RH without interpolation in this layer is less than 10%, (3) RH at all altitudes in this layer is less than 25%, and (4) Hybrid Single-Particles Lagrangian Integrated Trajectory (HYSPLIT) ensemble backward trajectories (Rolph, 2016; Stein et al., 2015) showing significant descending motion from near tropopause (empirically, 8 km is high enough for deep STT identification by considering modeling uncertainties) within the past 5 days. Based on our experience and some of previous studies (e.g., Sullivan et al., 2015), this 5 day duration is expected to cover the lifetime of most STT events with minimum misdiagnoses, although the air originating from the stratosphere could exist in the troposphere for more than 10 days without changing many of its characteristics (Bithell et al., 2000). For accurate identification, other important considerations are (1) with enhanced PV values (>0.5 PVU) and (2) with enhanced total column ozone shown by the satellite-borne Ozone Monitoring Instrument (OMI) (Levelt et al., 2006; Veefkind et al., 2006). The STT layer emphasizes the "irreversible" mixing of the stratospheric air into the troposphere. This process requires that the STT layer should be below the tropopause altitude; however, tropopause heights can be strongly dependent on the definition such as in the previously mentioned flight HU795 on July 13. PV is used only as an optional indicator instead of an exclusive criterion due to the calculation uncertainty arising from the model's temporal, spatial, and vertical resolutions. The STT feature could be small spatially so that there could be a geographical offset between observations and modeled products.

In the following analysis, the climatological monthly average is considered as the reference ozone amount without STT influence. An enhanced ozone layer is defined as a lamina where the ozone mixing ratio exceeds the ozone reference level by 5 ppbv. The University of Wisconsin's high spectral resolution lidar (HSRL) (Grund & Eloranta, 1991) was colocated with the ozone lidar from June to November 2013. The HSRL backscatter data are helpful to distinguish the elevated ozone due to biomass burning smoke from elevated ozone due to STT.

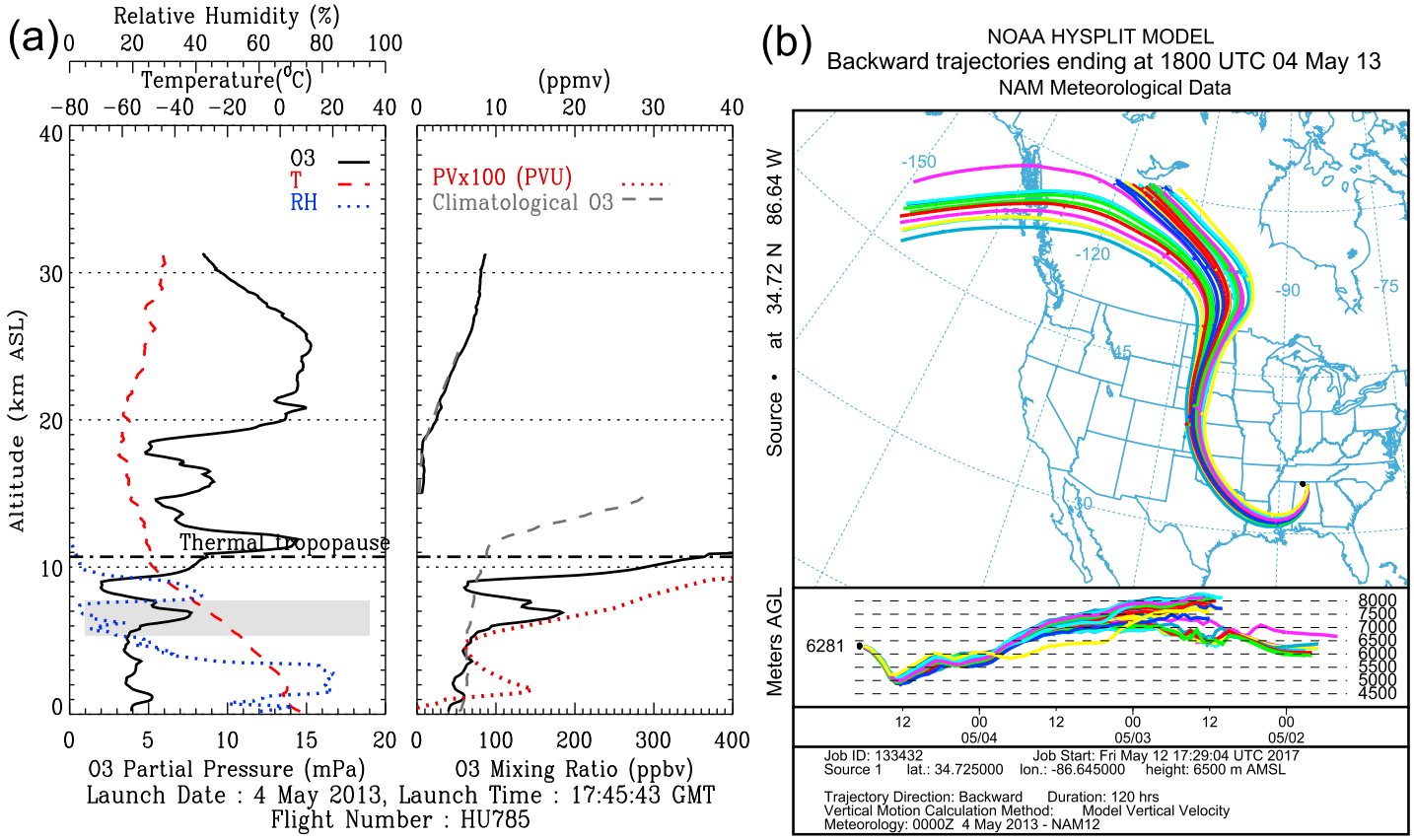

Figure 6. An example for the STT layer detection from the ozonesonde profiles. (a) The largest ozone enhanced layer in the study (in the gray area) occurred on 4 May 2013 between 5.3 and 7.7 km with peak ozone at 184 ppbv and minimum RH at 1.8%. (b) Five day HYSPLIT backward trajectory ensemble in Huntsville, supplied with the 12 km meteorological field from the North American Mesoscale model (Janjic, 2003), as well as the enhanced PV (>2 PVU) suggests the stratospheric origin for the 6.5 km layer.

Figure 6 shows an example of an STT layer on 4 May 2013 identified by the described algorithm. The maximum ozone in the layer, centered at 6.5 km, reaches 184 ppbv with a minimum RH of 1.8% and significantly enhanced PV. Ozone and RH are well anticorrelated in this layer. The thermal tropopause is located at 10.7 km, which is relatively low compared to the climatology. The moist layer with low ozone value (~60 ppbv) centered at 8.2 km suggests that the 6.5 km ozone layer has likely been mixed into the troposphere from the stratosphere. Despite a distinct laminar feature demonstrated by the ozonesonde profile, the PV profile does not display a laminar feature around 6.5 km probably because of the calculation uncertainty from the model's temporal and spatial resolutions. The HYSPLIT back trajectories in Figure 6b indicate a primarily cyclonic and descending flow for the 6.5 km layer except for a short-term ascending flow at the recent 6 h. The 1.3 km ozone enhanced layer possibly has stratospheric origin with enhanced PV. However, it is excluded as a STT layer because of high RH. Please note that the 1.3 km ozone layer was located above the PBL height at this time, about 1 km, suggested by the temperature inversion. After checking the hourly ozone data from the Environmental Protection Agency (not shown), we did not find any enhanced surface ozone event associated with the potential stratospheric influence for this case.

Table 1 gives the statistics of the identified STT layers for 13-May-Sep. The detected maximum ozone enhancement beyond the climatology below 9 km, due to the stratosphere influence, can be as high as 162% (114 ppbv) with an average enhancement of 52 ± 33% (35 ± 24 ppbv). The average enhancement is much higher than the detection threshold (25%). These layers are much drier than the predefined detection threshold (minimum RH = 10%) with a minimum RH varying between 0.3% and 6.3% at an average of 2.3 ± 1.7%. The large ozone enhancement and low RH reflect the persistent characteristics of stratospheric-sourced layers (Newell et al., 1999). STT layers are present at almost all altitudes above the PBL with a higher frequency between 5 and 7 km (Figure 7). The thickness of the layers is somewhat

Table 1
Statistics of Ozone Enhancement Below 9 km Due To the STT Process

Date	Flight number	Middle altitude	Thickness	Min RH (%)[a]	Background O3 (ppbv)	Max ΔO3 (ppbv)	Max ΔO3 (%)
May 4	785	6.5	2.4	1.8	70	114	162
May 11	786	7.1	1.2	6.3	70	50	71
Jun 1	789	5.9	1.6	0.3	65	32	49
Jun 8	790	3.6	1.8	0.7	62	22	35
Jun 29	793	4.8	1	2	62	35	56
Jul 13	795	6.95	0.9	3.7	72	19	26
Aug 16	806	8.3	1.4	5.4	82	38	46
Aug 17	807	6.95	3.7	2.5	79	63	80
Aug 19	808	5.25	2.3	2.9	73	18	25
		7.9	1.8	2	81	45	56
Aug 20	809	5.9	2.8	0.8	68	35	51
Aug 24	813	5.7	0.6	0.5	70	19	27
Sep 2	820	5.5	1.6	1.6	56	30	54
Sep 4	821	2.85	0.9	2.7	55	16	29
Sep 6	822	8.65	3.3	3.8	57	21	35
Sep 14	826	2.3	0.4	1	56	15	27
		6.35	2.3	1.9	56	31	55
Average		5.91	1.8	2.3		35	52
1σ standard deviation		1.78	0.9	1.7		24	33

[a]The minimum RH is unsmoothed, raw data.

related to its definition (Huang et al., 2015). From this study, the average thickness of the detected STT layers is 1.7 ± 0.9 km.

The average STT layer occurrence frequency for these months (Table 2) is 31%. Tropopause folding, the most important mechanism for STT (Sprenger et al., 2003), occurs predominantly at midlatitudes, approximately between 40° and 60° according to Liang et al. (2009); however, it eventually affects the subtropics through quasi-isentropic descent (Kuang et al., 2012, 2017). According to Sprenger & Wernli (2003), the STT events that affect the tropospheric ozone in SEUS primarily originate from the cross-tropopause flux over British Columbia, Canada, and the northwestern U.S. The deep STT where the stratospheric intrusion affects altitudes below 3 km accounts for 13% of all the detected layers. The deep STT detection is related to the chosen detection algorithm and may have higher uncertainty because the longer the stratospheric air stays in the troposphere, the more likely it will lose its original characteristics through mixing.

The monthly change of STT layer occurrence rates, relatively high in May and June with significant reduction in later months, is consistent with previous modeling studies (Liang et al., 2009; Sprenger & Wernli, 2003). Although the sample size is small, the high frequencies of STT layers for May and June 2013 explain the positive ozone anomalies in the middle and lower troposphere during these 2 months. Note the detection range for this work is midtroposphere and PBL, so the results for detection rates cannot be compared to the studies using surface data (Stohl et al., 2000). None of the STT layers in the PBL were identified during 13-May-Sep, likely because layers lose their laminar characteristics after mixing into the PBL from free troposphere (FT). Therefore, further quantification of the STT influence on the surface in SEUS may require both accurate trajectory tracking of air parcel (Wernli & Bourqui, 2002) and careful parametrization of the PBL mixing scheme (Pleim, 2007). Because of significant topographic differences, the stratospheric influence on the surface ozone is more frequently observed in the western U.S. than in SEUS (Lefohn et al., 2012; Lin et al., 2012; Ott et al., 2016).

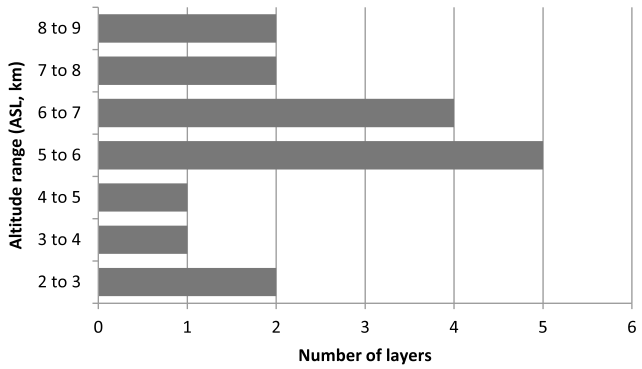

Figure 7. Altitude distribution of number of STT layers.

Characterization of the stratospheric contribution to tropospheric ozone can improve satellite retrievals of vertical ozone profiles (Moody et al., 2012) which are largely based on a priori information.

Table 2
STT Occurrence Frequency in Percentage

	May	June	July	August	September	All
Number of profiles with detected STT	2	3	1	5	4	15
Total profiles	4	5	4	22	13	48
Detection frequency	50%	60%	25%	23%	31%	31%

When the actual shape of the ozone profile deviates significantly from the climatological mean especially under a relatively small-scale weather system, knowledge of the nonclimatological ozonesonde profiles is helpful in obtaining accurate satellite retrievals.

6. Summary and Conclusions

The 48 ozonesonde observations made at Huntsville during the ozone season, from May to September, in 2013 measure 10 ppbv (about 17%) lower than the climatology in the PBL, close to the climatology in the midtroposphere, and 40 ppbv (about 25%) higher than the climatology in the upper troposphere (Figure 2). The low ozone in the PBL, especially in July and August, is closely associated with the unusually wet and cool weather during these months in Huntsville. The coherent enhanced ozone and PV as well as the large variability in the UTLS in May, June, and July (Figure 3) suggest a strong influence of the lower stratosphere on the upper troposphere during these months.

This study demonstrates that the upper air ozone generally increases with increasing temperature or decreasing RH, similar to the surface (Camalier et al., 2007; Dueñas et al., 2002). Quantifying the correlation of anomalies between ozone and RH in four altitude regions: surface, PBL, midtroposphere (PBL top —9 km), and upper troposphere (9 km—tropopause) reveals that the ozone anomalies are strongly anticorrelated with RH anomalies for all the altitude regions with r of about 0.6 (Figure 5). The ozone/RH regression slopes are −1.0, −0.6, −0.5, and −3.6 ppbv·%$^{-1}$ for surface, PBL, midtroposphere, and upper troposphere, respectively. The ozone anomalies are strongly correlated with the temperature anomalies within the troposphere (r = about 0.6) except for the midtroposphere (r = 0.4). The regression slopes between ozone and temperature anomalies for surface, PBL, and midtroposphere are similar, 3.0–4.1 ppbv K^{-1} consistent with previous studies using surface air quality data (Olszyna et al., 1997; Rasmussen et al., 2012). The ozone/temperature slope for upper troposphere is 28.0 ppbv K^{-1}, significantly distinct from lower altitudes due to stratospheric influences. These results will be valuable for correctly accounting for meteorological adjustment of ozone concentration when examining ozone trends (Lin et al., 2014) and for improving the accuracy in evaluation of the effect of climate change on tropospheric ozone (Jacob & Winner, 2009).

We have quantified the stratospheric influence on the midtropospheric and PBL ozone with a laminar identification method using the criteria of peak ozone, RH value, and the back trajectory analysis. The detected layers have a mean maximum ozone enhancement over the climatology of 52 ± 33% (35 ± 24 ppbv) with a mean minimum RH of 2.3 ± 1.7% due to stratospheric influence. This result suggests the STT layers remain extremely dry after descent, although the ozone mixing ratio diminishes compared to the original stratospheric air consistent with previous results (Trickl et al., 2014). The STT occurrence frequency is much higher in May and June (≥50%) than July, August, and September (~30%) reflecting the seasonal STT flux variation for the Northern Hemisphere (Liang et al., 2009). The deep STT, affecting altitudes below 3 km, accounts for 13% of all the detected layers. This study indicates that the stratospheric influence on FT ozone could be significant in the SEUS during early summer (Thompson et al., 2015; Yorks et al., 2009). Our detection method did not identify any STT layers within the PBL. Because laminar characteristics are difficult to maintain under strong mixing conditions, the lifetimes of laminae in this regime are expected to be quite short. For this reason, further modeling analysis (Johnson et al., 2016; Lin et al., 2012) is needed to quantify the role of stratospheric influence on the surface ozone in the SEUS.

Acknowledgments
We would like to thank the UAH ozonesonde group, including the current and former UAH students, for the high-quality measurements they made overtime during weekend. We thank Edwin W. Eloranta for providing the HSRL aerosol data, the NOAA Air Resources Laboratory (ARL) for providing the HYSPLIT modeled trajectory data (http://ready.arl.noaa.gov), and the Royal Netherlands Meteorological Institute (KNMI) for providing the archived OMI column ozone data (http://www.temis.nl/protocols/O3total.html) used in this publication. This work is supported by TOLNet (NNX15AD37G) and SEAC^{4}RS (NNX13AL89G) programs. The 2013 ozonesonde data used in this study are archived both at http://www.nsstc.uah.edu/public/lidar/archive/Ozonesonde/2013/ and the SEACIONS network (http://ozone.met.psu.edu/dev/research/seacions/quicklooks.php) sponsored by NOAA, NASA/GSFC, and Penn State University with grant code of NNX12AF05G. The views, opinions, and findings contained in this report are those of the authors and should not be construed as an official NOAA, NASA, or U.S. Government position, policy, or decision.

References

Beekmann, M., Ancellet, G., Blonsky, S., De Muer, D., Ebel, A., Elbern, H., … Van Haver, P. (1997). Regional and global tropopause fold occurrence and related ozone flux across the tropopause. *Journal of Atmospheric Chemistry*, *28*(1/3), 29–44. https://doi.org/10.1023/A:1005897314623

Bethan, S., Vaughan, G., & Reid, S. J. (1996). A comparison of ozone and thermal tropopause heights and the impact of tropopause definition on quantifying the ozone content of the troposphere. *Quarterly Journal of the Royal Meteorological Society*, *122*(532), 929–944. https://doi.org/10.1002/qj.49712253207

Bithell, M., Vaughan, G., & Gray, L. J. (2000). Persistence of stratospheric ozone layers in the troposphere. *Atmospheric Environment*, *34*(16), 2563–2570. https://doi.org/10.1016/S1352-2310(99)00497-5

Bloomer, B. J., Stehr, J. W., Piety, C. A., Salawitch, R. J., & Dickerson, R. R. (2009). Observed relationships of ozone air pollution with temperature and emissions. *Geophysical Research Letters*, *36*, L09803. https://doi.org/10.1029/2009GL037308

Blunden, J., & Arndt, D. S. (Eds) (2014). State of the climate in 2013. *Bulletin of the American Meteorological Society*, *95*(7), S1–S279. https://doi.org/10.1175/2014BAMSStateoftheClimate.1

Bourqui, M. S., & Trépanier, P.-Y. (2010). Descent of deep stratospheric intrusions during the IONS August 2006 campaign. *Journal of Geophysical Research*, *115*, D18301. https://doi.org/10.1029/2009JD013183

Bourqui, M. S., Yamamoto, A., Tarasick, D., Moran, M. D., Beaudoin, L.-P., Beres, I., … Wilkinson, R. (2012). A new real-time Lagrangian diagnostic system for stratosphere-troposphere exchange: Evaluation during a balloon sonde campaign in eastern Canada. *Atmospheric Chemistry and Physics*, *12*(5), 2661–2679. https://doi.org/10.5194/acp-12-2661-2012

Camalier, L., Cox, W., & Dolwick, P. (2007). The effects of meteorology on ozone in urban areas and their use in assessing ozone trends. *Atmospheric Environment*, *41*(33), 7127–7137. https://doi.org/10.1016/j.atmosenv.2007.04.061

Cooper, O. R., Trainer, M., Thompson, A. M., Oltmans, S. J., Tarasick, D. W., Witte, J. C., … Minschwaner, K. (2007). Evidence for a recurring eastern North America upper tropospheric ozone maximum during summer. *Journal of Geophysical Research*, *112*, D23304. https://doi.org/10.1029/2007JD008710

Cox, W. M., & Chu, S. H. (1996). Assessment of interannual ozone variation in urban areas from a climatological perspective. *Atmospheric Environment*, *30*(14), 2615–2625. https://doi.org/10.1016/1352-2310(95)00346-0

Danielsen, E. F. (1968). Stratospheric-tropospheric exchange based on radioactivity, ozone and potential vorticity. *Journal of the Atmospheric Sciences*, *25*(3), 502–518. https://doi.org/10.1175/1520-0469(1968)025%3C0502:STEBOR%3E2.0.CO;2

DeCaria, A. J., Pickering, K. E., Stenchikov, G. L., & Ott, L. E. (2005). Lightning-generated NO_X and its impact on tropospheric ozone production: A three-dimensional modeling study of a Stratosphere-Troposphere Experiment: Radiation, Aerosols and Ozone (STERAO-A) thunderstorm. *Journal of Geophysical Research*, *110*, D14303. https://doi.org/10.1029/2004JD005556

Dee, D. P., Uppala, S. M., Simmons, A. J., Berrisford, P., Poli, P., Kobayashi, S., … Vitart, F. (2011). The ERA-Interim reanalysis: Configuration and performance of the data assimilation system. *Quarterly Journal of the Royal Meteorological Society*, *137*(656), 553–597. https://doi.org/10.1002/qj.828

Dickerson, R. R., Huffman, G. J., & Luke, W. T. (1987). Thunderstorms: An important mechanism in the transport of air pollutants. *Science*, *235*(4787), 460–465. https://doi.org/10.1126/science.235.4787.460

Dueñas, C., Fernández, M. C., Cañete, S., Carretero, J., & Liger, E. (2002). Assessment of ozone variations and meteorological effects in an urban area in the Mediterranean Coast. *Science of the Total Environment*, *299*(1–3), 97–113. https://doi.org/10.1016/S0048-9697(02)00251-6

Elbern, H., Kowol, J., Sladkovic, R., & Ebel, A. (1997). Deep stratospheric intrusions: A statistical assessment with model guided analyses. *Atmospheric Environment*, *31*(19), 3207–3226. https://doi.org/10.1016/S1352-2310(97)00063-0

Fusco, A. C., & Logan, J. A. (2003). Analysis of 1970–1995 trends in tropospheric ozone at Northern Hemisphere midlatitudes with the GEOS-CHEM model. *Journal of Geophysical Research*, *108*(D15), 4449. doi:https://doi.org/10.1029/2002JD002742

Grund, C. J., & Eloranta, E. W. (1991). University of Wisconsin high spectral resolution lidar. *Optical Engineering*, *30*(1), 6–12. https://doi.org/10.1117/12.55766

Hess, P. G., & Zbinden, R. (2013). Stratospheric impact on tropospheric ozone variability and trends: 1990–2009. *Atmospheric Chemistry and Physics*, *13*(2), 649–674. https://doi.org/10.5194/acp-13-649-2013

Hidy, G. M., Blanchard, C. L., Baumann, K., Edgerton, E., Tanenbaum, S., Shaw, S., … Walters, J. (2014). Chemical climatology of the southeastern United States, 1999–2013. *Atmospheric Chemistry and Physics*, *14*(21), 11,893–11,914. https://doi.org/10.5194/acp-14-11893-2014

Homeyer, C. R., Bowman, K. P., Pan, L. L., Atlas, E. L., Gao, R.-S., & Campos, T. L. (2011). Dynamical and chemical characteristics of tropospheric intrusions observed during START08. *Journal of Geophysical Research*, *116*, D06111. https://doi.org/10.1029/2010JD015098

Huang, G., Newchurch, M. J., Kuang, S., Buckley, P. I., Cantrell, W., & Wang, L. (2015). Definition and determination of ozone laminae using continuous Wavelet Transform (CWT) analysis. *Atmospheric Environment*, *104*, 125–131. https://doi.org/10.1016/j.atmosenv.2014.12.027

Hurst, D. F., Hall, E. G., Jordan, A. F., Miloshevich, L. M., Whiteman, D. N., Leblanc, T., … Oltmans, S. J. (2011). Comparisons of temperature, pressure and humidity measurements by balloon-borne radiosondes and frost point hygrometers during MOHAVE-2009. *Atmospheric Measurement Techniques*, *4*(12), 2777–2793. https://doi.org/10.5194/amt-4-2777-2011

Im, U., Markakis, K., Poupkou, A., Melas, D., Unal, A., Gerasopoulos, E., … Kanakidou, M. (2011). The impact of temperature changes on summer time ozone and its precursors in the Eastern Mediterranean. *Atmospheric Chemistry and Physics*, *11*(8), 3847–3864. https://doi.org/10.5194/acp-11-3847-2011

Jacob, D. J. (2000). Heterogeneous chemistry and tropospheric ozone. *Atmospheric Environment*, *34*(12–14), 2131–2159. https://doi.org/10.1016/S1352-2310(99)00462-8

Jacob, D. J., & Winner, D. A. (2009). Effect of climate change on air quality. *Atmospheric Environment*, *43*(1), 51–63. https://doi.org/10.1016/j.atmosenv.2008.09.051

Janjic, Z. I. (2003). A nonhydrostatic model based on a new approach. *Meteorology and Atmospheric Physics*, *82*(1–4), 271–285. https://doi.org/10.1007/s00703-001-0587-6

Johnson, B. J., Helmig, D., & Oltmans, S. J. (2008). Evaluation of ozone measurements from a tethered balloon-sampling platform at South Pole Station in December 2003. *Atmospheric Environment*, *42*(12), 2780–2787. https://doi.org/10.1016/j.atmosenv.2007.03.043

Johnson, M. S., Kuang, S., Wang, L., & Newchurch, M. J. (2016). Evaluating summer-time ozone enhancement events in the southeast United States. *Atmosphere*, *7*(8), 108. https://doi.org/10.3390/atmos7080108

Johnson, B. J., Oltmans, S. J., Vömel, H., Smit, H. G. J., Deshler, T., & Kroger, C. (2002). Electrochemical concentration cell (ECC) ozonesonde pump efficiency measurements and tests on the sensitivity to ozone of buffered and unbuffered ECC sensor cathode solutions. *Journal of Geophysical Research*, *107*(D19), 4393. https://doi.org/10.1029/2001JD000557

Komhyr, W. D. (1969). Electrochemical cells for gas analysis. *Annales de Geophysique*, *25*, 203–210.

Komhyr, W. D., Barnes, R. A., Brothers, G. B., Lathrop, J. A., & Opperman, D. P. (1995). Electrochemical concentration cell ozonesonde performance evaluation during STOIC 1989. *Journal of Geophysical Research*, *100*(D5), 9231–9244. https://doi.org/10.1029/94JD02175

Kuang, S., Newchurch, M. J., Burris, J., Wang, L., Buckley, P., Johnson, S., … Phillips, D. (2011). Nocturnal ozone enhancement in the lower troposphere observed by lidar. *Atmospheric Environment*, *45*(33), 6078–6084. https://doi.org/10.1016/j.atmosenv.2011.07.038

Kuang, S., Newchurch, M. J., Burris, J., Wang, L., Knupp, K., & Huang, G. (2012). Stratosphere-to-troposphere transport revealed by ground-based lidar and ozonesonde at a midlatitude site. *Journal of Geophysical Research*, *117*, D18305. https://doi.org/10.1029/2012JD017695

Kuang, S., Newchurch, M. J., Johnson, M. S., Wang, L., Burris, J., Pierce, R. B., … Feng, N. (2017). Summertime tropospheric ozone enhancement associated with a cold front passage due to stratosphere-to-troposphere transport and biomass burning: Simultaneous ground-based lidar and airborne measurements. *Journal of Geophysical Research: Atmospheres*, *122*, 1293–1311. https://doi.org/10.1002/2016JD026078

Langford, A. O., Brioude, J., Cooper, O. R., Senff, C. J., Alvarez, R. J. II, Hardesty, R. M., … Oltmans, S. J. (2012). Stratospheric influence on surface ozone in the Los Angeles area during late spring and early summer of 2010. *Journal of Geophysical Research*, *117*, D00V06. https://doi.org/10.1029/2011JD016766

Lefohn, A. S., Emery, C., Shadwick, D., Wernli, H., Jung, J., & Oltmans, S. J. (2014). Estimates of background surface ozone concentrations in the United States based on model-derived source apportionment. *Atmospheric Environment*, *84*, 275–288. https://doi.org/10.1016/j.atmosenv.2013.11.033

Lefohn, A. S., Wernli, H., Shadwick, D., Oltmans, S. J., & Shapiro, M. (2012). Quantifying the importance of stratospheric-tropospheric transport on surface ozone concentrations at high- and low-elevation monitoring sites in the United States. *Atmospheric Environment*, *62*, 646–656. https://doi.org/10.1016/j.atmosenv.2012.09.004

Lelieveld, J., & Dentener, F. J. (2000). What controls tropospheric ozone? *Journal of Geophysical Research*, *105*(D3), 3531–3551. https://doi.org/10.1029/1999JD901011

Levelt, P. F., van den Oord, G. H. J., Dobber, M. R., Mälkki, A., Visser, H., de Vries, J., … Saari, H. (2006). The ozone monitoring instrument. *IEEE Transactions on Geoscience and Remote Sensing*, *44*(5), 1093–1101. https://doi.org/10.1109/TGRS.2006.872333

Li, Q., Jacob, D. J., Park, R., Wang, Y., Heald, C. L., Hudman, R., … Evans, M. (2005). North American pollution outflow and the trapping of convectively lifted pollution by upper-level anticyclone. *Journal of Geophysical Research*, *110*, D10301. https://doi.org/10.1029/2004JD005039

Liang, Q., Douglass, A. R., Duncan, B., Stolarski, R., & Witte, J. (2009). The governing processes and timescales of stratosphere-to-troposphere transport and its contribution to ozone in the Arctic troposphere. *Atmospheric Chemistry and Physics*, *9*(9), 3011–3025. https://doi.org/10.5194/acp-9-3011-2009

Lin, M., Fiore, A. M., Cooper, O. R., Horowitz, L. W., Langford, A. O., Levy, H. II, … Senff, C. J. (2012). Springtime high surface ozone events over the western United States: Quantifying the role of stratospheric intrusions. *Journal of Geophysical Research*, *117*, D00V22. https://doi.org/10.1029/2012JD018151

Lin, M., Horowitz, L. W., Oltmans, S. J., Fiore, A. M., & Fan, S. (2014). Tropospheric ozone trends at Mauna Loa Observatory tied to decadal climate variability. *Nature Geoscience*, *7*(2), 136–143. https://doi.org/10.1038/ngeo2066

Logan, J. A., Jones, D. B. A., Megretskaia, I. A., Oltmans, S. J., Johnson, B. J., Vömel, H., … Schmidlin, F. J. (2003). Quasibiennial oscillation in tropical ozone as revealed by ozonesonde and satellite data. *Journal of Geophysical Research*, *108*(D8), 4244. https://doi.org/10.1029/2002JD002170

Miloshevich, L. M., Vömel, H., Whiteman, D. N., Lesht, B. M., Schmidlin, F. J., & Russo, F. (2006). Absolute accuracy of water vapor measurements from six operational radiosonde types launched during AWEX-G and implications for AIRS validation. *Journal of Geophysical Research*, *111*, D09S10. https://doi.org/10.1029/2005JD006083

Monks, P. S. (2000). A review of the observations and origins of the spring ozone maximum. *Atmospheric Environment*, *34*(21), 3545–3561. https://doi.org/10.1016/S1352-2310(00)00129-1

Moody, J. L., Felker, S. R., Wimmers, A. J., Osterman, G., Bowman, K., Thompson, A. M., & Tarasick, D. W. (2012). A multi-sensor upper tropospheric ozone product (MUTOP) based on TES ozone and GOES water vapor: Validation with ozonesondes. *Atmospheric Chemistry and Physics*, *12*(12), 5661–5676. https://doi.org/10.5194/acp-12-5661-2012

Morris, G. A., Ford, B., Rappenglück, B., Thompson, A. M., Mefferd, A., Ngan, F., & Lefer, B. (2010). An evaluation of the interaction of morning residual layer and afternoon mixed layer ozone in Houston using ozonesonde data. *Atmospheric Environment*, *44*(33), 4024–4034. https://doi.org/10.1016/j.atmosenv.2009.06.057

Nassar, R., Logan, J. A., Worden, H. M., Megretskaia, I. A., Bowman, K. W., Osterman, G. B., … Witte, J. C. (2008). Validation of Tropospheric Emission Spectrometer (TES) nadir ozone profiles using ozonesonde measurements. *Journal of Geophysical Research*, *113*, D15S17. https://doi.org/10.1029/2007JD008819

Neu, J. L., Flury, T., Manney, G. L., Santee, M. L., Livesey, N. J., & Worden, J. (2014). Tropospheric ozone variations governed by changes in stratospheric circulation. *Nature Geoscience*, *7*(5), 340–344. https://doi.org/10.1038/ngeo2138

Newchurch, M. J., Ayoub, M. A., Oltmans, S., Johnson, B., & Schmidlin, F. J. (2003). Vertical distribution of ozone at four sites in the United States. *Journal of Geophysical Research*, *108*(D1), 4031. https://doi.org/10.1029/2002JD002059

Newell, R. E., Thouret, V., Cho, J. Y., Stoller, P., Marenco, A., & Smit, H. G. (1999). Ubiquity of quasi-horizontal layers in the troposphere. *Nature*, *398*(6725), 316–319. https://doi.org/10.1038/18642

Olszyna, K. J., Luria, M., & Meagher, J. F. (1997). The correlation of temperature and rural ozone levels in southeastern U.S.A. *Atmospheric Environment*, *31*(18), 3011–3022. https://doi.org/10.1016/S1352-2310(97)00097-6

Ott, L. E., Duncan, B. N., Thompson, A. M., Diskin, G., Fasnacht, Z., Langford, A. O., … Yasuko, Y. (2016). Frequency and impact of summertime stratospheric intrusions over Maryland during DISCOVER-AQ (2011): New evidence from NASA's GEOS-5 simulations. *Journal of Geophysical Research: Atmospheres*, *121*, 3687–3706. https://doi.org/10.1002/2015JD024052

Pan, L. L., Randel, W. J., Gary, B. L., Mahoney, M. J., & Hintsa, E. J. (2004). Definitions and sharpness of the extratropical tropopause: A trace gas perspective. *Journal of Geophysical Research*, *109*, D23103. https://doi.org/10.1029/2004JD004982

Pleim, J. E. (2007). A combined local and nonlocal closure model for the atmospheric boundary layer. Part II: Application and evaluation in a mesoscale meteorological model. *Journal of Applied Meteorology and Climatology*, *46*(9), 1396–1409. https://doi.org/10.1175/JAM2534.1

Randel, W. J., & Cobb, J. B. (1994). Coherent variations of monthly mean total ozone and lower stratospheric temperature. *Journal of Geophysical Research*, *99*(D3), 5433–5447. https://doi.org/10.1029/93JD03454

Rasmussen, D. J., Fiore, A. M., Naik, V., Horowitz, L. W., McGinnis, S. J., & Schultz, M. G. (2012). Surface ozone-temperature relationships in the eastern US: A monthly climatology for evaluating chemistry-climate models. *Atmospheric Environment*, *47*, 142–153. https://doi.org/10.1016/j.atmosenv.2011.11.021

Reed, R. J. (1950). The role of vertical motions in ozone-weather relationships. *Journal of Meteorology*, *7*(4), 263–267. https://doi.org/10.1175/1520-0469(1950)007%3C0263:TROVMI%3E2.0.CO;2

Reid, J. S., Kuehn, R. E., Holz, R. E., Eloranta, E. W., Kaku, K. C., Kuang, S., & Newchurch, M. J. (2017). Ground based high spectral resolution lidar observation of aerosol vertical distribution in the summertime Southeast United States. *Journal of Geophysical Research: Atmospheres*, *122*, 2970–3004. https://doi.org/10.1002/2016JD025798

Ren, X., Olson, J. R., Crawford, J. H., Brune, W. H., Mao, J., Long, R. B., … Shetter, R. E. (2008). HO_x chemistry during INTEX-A 2004: Observation, model calculation, and comparison with previous studies. *Journal of Geophysical Research*, *113*, D05310. https://doi.org/10.1029/2007JD009166

Rolph, G. D. (2016). Real-Time Environmental Applications and Display SYstem (READY). Park, MD: NOAA Air Resources Laboratory, College. Retrieved from http://www.ready.noaa.gov

Seidel, D. J., Ross, R. J., Angell, J. K., & Reid, G. C. (2001). Climatological characteristics of the tropical tropopause as revealed by radiosondes. *Journal of Geophysical Research*, *106*(D8), 7857–7878. https://doi.org/10.1029/2000JD900837

Škerlak, B., Sprenger, M., & Wernli, H. (2014). A global climatology of stratosphere-troposphere exchange using the ERA-Interim data set from 1979 to 2011. *Atmospheric Chemistry and Physics*, *14*(2), 913–937. https://doi.org/10.5194/acp-14-913-2014

Smit, H. G. J., Straeter, W., Johnson, B. J., Oltmans, S. J., Davies, J., Tarasick, D. W., … Posny, F. (2007). Assessment of the performance of ECC-ozonesondes under quasi-flight conditions in the environmental simulation chamber: Insights from the Juelich Ozone Sonde Intercomparison Experiment (JOSIE). *Journal of Geophysical Research*, *112*, D19306. https://doi.org/10.1029/2006JD007308

Sprenger, M., Croci Maspoli, M., & Wernli, H. (2003). Tropopause folds and cross-tropopause exchange: A global investigation based upon ECMWF analyses for the time period March 2000 to February 2001. *Journal of Geophysical Research*, *108*(D12), 8518. https://doi.org/10.1029/2002JD002587

Sprenger, M., & Wernli, H. (2003). A northern hemispheric climatology of cross-tropopause exchange for the ERA15 time period (1979–1993). *Journal of Geophysical Research*, *108*(D12), 8521. https://doi.org/10.1029/2002JD002636

Stauffer, R. M., Morris, G. A., Thompson, A. M., Joseph, E., Coetzee, G. J., & Nalli, N. R. (2014). Propagation of radiosonde pressure sensor errors to ozonesonde measurements. *Atmospheric Measurement Techniques*, *7*(1), 65–79. https://doi.org/10.5194/amt-7-65-2014

Stauffer, R. M., Thompson, A. M., Oltmans, S. J., & Johnson, B. J. (2017). Tropospheric ozonesonde profiles at long-term U.S. monitoring sites: 2. Links between Trinidad Head, CA, profile clusters and inland surface ozone measurements. *Journal of Geophysical Research: Atmospheres*, *122*, 1261–1280. https://doi.org/10.1002/2016JD025254

Stauffer, R. M., Thompson, A. M., & Young, G. S. (2016). Tropospheric ozonesonde profiles at long-term U.S. monitoring sites: 1. A climatology based on self-organizing maps. *Journal of Geophysical Research: Atmospheres*, *121*, 1320–1339. https://doi.org/10.1002/2015JD023641

Stein, A. F., Draxler, R. R., Rolph, G. D., Stunder, B. J. B., Cohen, M. D., & Ngan, F. (2015). NOAA's HYSPLIT atmospheric transport and dispersion modeling system. *Bulletin of the American Meteorological Society*, *96*(12), 2059–2077. https://doi.org/10.1175/BAMS-D-14-00110.1

Steinbrecht, W., Claude, H., Schönenborn, F., Leiterer, U., Dier, H., & Lanzinger, E. (2008). Pressure and temperature differences between Vaisala RS80 and RS92 radiosonde systems. *Journal of Atmospheric and Oceanic Technology*, *25*(6), 909–927. https://doi.org/10.1175/2007JTECHA999.1

Steinbrecht, W., Hassler, B., Claude, H., Winkler, P., & Stolarski, R. S. (2003). Global distribution of total ozone and lower stratospheric temperature variations. *Atmospheric Chemistry and Physics*, *3*(5), 1421–1438. https://doi.org/10.5194/acp-3-1421-2003

Stohl, A., Spichtinger-Rakowsky, N., Bonasoni, P., Feldmann, H., Memmesheimer, M., Scheel, H. E., … Mandl, M. (2000). The influence of stratospheric intrusions on alpine ozone concentrations. *Atmospheric Environment*, *34*(9), 1323–1354. https://doi.org/10.1016/S1352-2310(99)00320-9

Sudo, K., Takahashi, M., & Akimoto, H. (2003). Future changes in stratosphere-troposphere exchange and their impacts on future tropospheric ozone simulations. *Geophysical Research Letters*, *30*(24), 2256. https://doi.org/10.1029/2003GL018526

Sullivan, J. T., McGee, T. J., Thompson, A. M., Pierce, R. B., Sumnicht, G. K., Twigg, L. W., … Hoff, R. M. (2015). Characterizing the lifetime and occurrence of stratospheric-tropospheric exchange events in the rocky mountain region using high-resolution ozone measurements. *Journal of Geophysical Research: Atmospheres*, *120*, 12,410–12,424. https://doi.org/10.1002/2015JD023877

Tarasick, D. W., Moran, M. D., Thompson, A. M., Carey-Smith, T., Rochon, Y., Bouchet, V. S., … Joseph, E. (2007). Comparison of Canadian air quality forecast models with tropospheric ozone profile measurements above midlatitude North America during the IONS/ICARTT campaign: Evidence for stratospheric input. *Journal of Geophysical Research*, *112*, D12S22. https://doi.org/10.1029/2006JD007782

Terao, Y., Logan, J. A., Douglass, A. R., & Stolarski, R. S. (2008). Contribution of stratospheric ozone to the interannual variability of tropospheric ozone in the northern extratropics. *Journal of Geophysical Research*, *113*, D18309. https://doi.org/10.1029/2008JD009854

Thompson, A. M., Oltmans, S. J., Tarasick, D. W., von der Gathen, P., Smit, H. G., & Witte, J. C. (2011). Strategic ozone sounding networks: Review of design and accomplishments. *Atmospheric Environment*, *45*(13), 2145–2163. https://doi.org/10.1016/j.atmosenv.2010.05.002

Thompson, A. M., Stauffer, R. M., Miller, S. K., Martins, D. K., Joseph, E., Weinheimer, A. J., & Diskin, G. S. (2015). Ozone profiles in the Baltimore-Washington region (2006–2011): Satellite comparisons and DISCOVER-AQ observations. *Journal of Atmospheric Chemistry*, *72*(3-4), 393–422. https://doi.org/10.1007/s10874-014-9283-z

Thompson, A. M., Stone, J. B., Witte, J. C., Miller, S. K., Oltmans, S. J., Kucsera, T. L., … Ross, K. L. (2007). Intercontinental Chemical Transport Experiment Ozonesonde Network Study (IONS) 2004: 2. Tropospheric ozone budgets and variability over northeastern North America. *Journal of Geophysical Research*, *112*(D12), D12S13. https://doi.org/10.1029/2006JD007670

Thompson, A. M., Yorks, J. E., Miller, S. K., Witte, J. C., Dougherty, K. M., Morris, G. A., … Rappenglueck, B. (2008). Tropospheric ozone sources and wave activity over Mexico City and Houston during MILAGRO/Intercontinental Transport Experiment (INTEX-B) Ozonesonde Network Study, 2006 (IONS-06). *Atmospheric Chemistry*, *8*(17), 5113–5125. https://doi.org/10.5194/acp-8-5113-2008

Toon, O. B., Maring, H., Dibb, J., Ferrare, R., Jacob, D. J., Jensen, E. J., … Pszenny, A. (2016). Planning, implementation, and scientific goals of the Studies of Emissions and Atmospheric Composition, Clouds and Climate Coupling by Regional Surveys (SEAC4RS) field mission. *Journal of Geophysical Research: Atmospheres*, *121*, 4967–5009. https://doi.org/10.1002/2015JD024297

Travis, K. R., Jacob, D. J., Fisher, J. A., Kim, P. S., Marais, E. A., Zhu, L., … Zhou, X. (2016). Why do models overestimate surface ozone in the Southeast United States? *Atmospheric Chemistry and Physics*, *16*(21), 13,561–13,577. https://doi.org/10.5194/acp-16-13561-2016

Trickl, T., Vogelmann, H., Giehl, H., Scheel, H. E., Sprenger, M., & Stohl, A. (2014). How stratospheric are deep stratospheric intrusions?. *Atmospheric Chemistry and Physics*, *14*(18), 9941–9961. https://doi.org/10.5194/acp-14-9941-2014

Veefkind, J. P., de Haan, J. F., Brinksma, E. J., Kroon, M., & Levelt, P. F. (2006). Total ozone from the Ozone Monitoring Instrument (OMI) using the DOAS technique. *IEEE Transactions on Geoscience and Remote Sensing*, *44*(5), 1239–1244. https://doi.org/10.1109/TGRS.2006.871204

Vukovich, F. M., & Sherwell, J. (2003). An examination of the relationship between certain meteorological parameters and surface ozone variations in the Baltimore–Washington corridor. *Atmospheric Environment*, *37*(7), 971–981. https://doi.org/10.1016/S1352-2310(02)00994-9

Wang, J., Cole, H. L., Carlson, D. J., Miller, E. R., Beierle, K., Paukkunen, A., & Laine, T. K. (2002). Corrections of humidity measurement errors from the Vaisala RS80 radiosonde—Application to TOGA COARE data. *Journal of Atmospheric and Oceanic Technology*, *19*(7), 981–1002. https://doi.org/10.1175/1520-0426(2002)019%3C0981:COHMEF%3E2.0.CO;2

Wang, L., Cook, M., Newchurch, M. J., Pickering, K., Pour-Biazar, A., Kuang, S., … Peterson, H. (2015). Tropospheric ozone lidar data evaluation of the lightning-induced ozone enhancement simulated by the WRF/Chem model. *Atmospheric Environment*, *115*, 185–191. https://doi.org/10.1016/j.atmosenv.2015.05.054

Wang, L., Newchurch, M. J., Biazar, A., Liu, X., Kuang, S., & Khan, M. (2011). Evaluating AURA/OMI ozone profiles using Ozonesonde data and EPA surface measurements for August 2006. *Atmospheric Environment*, *45*(31), 5523–5530. https://doi.org/10.1016/j.atmosenv.2011.06.012

Warneke, C., Trainer, M., de Gouw, J. A., Parrish, D. D., Fahey, D. W., Ravishankara, A. R., … Hatch, C. D. (2016). Instrumentation and measurement strategy for the NOAA SENEX aircraft campaign as part of the Southeast Atmosphere Study 2013. *Atmospheric Measurement Techniques*, *9*(7), 3063–3093. https://doi.org/10.5194/amt-9-3063-2016

Wernli, H., & Bourqui, M. (2002). A Lagrangian "1-year climatology" of (deep) cross-tropopause exchange in the extratropical Northern Hemisphere. *Journal of Geophysical Research*, *107*(D2), 4021. https://doi.org/10.1029/2001JD000812

Wirth, V. (2000). Thermal versus dynamical tropopause in upper-tropospheric balanced flow anomalies. *Quarterly Journal of the Royal Meteorological Society*, *126*(562), 299–317. https://doi.org/10.1002/qj.49712656215

Wise, E. K., & Comrie, A. C. (2005). Meteorologically adjusted urban air quality trends in the southwestern United States. *Atmospheric Environment*, *39*(16), 2969–2980. https://doi.org/10.1016/j.atmosenv.2005.01.024

World Meteorological Organization (WMO) (1986). Atmospheric ozone 1985, WMO Global Ozone Res. and Monit. Proj. Rep. 20, Geneva, Switzerland.

Yorks, J. E., Thompson, A. M., Joseph, E., & Miller, S. K. (2009). The variability of free tropospheric ozone over Beltsville, Maryland (39N, 77W) in the summers 2004–2007. *Atmospheric Environment*, *43*(11), 1827–1838. https://doi.org/10.1016/j.atmosenv.2008.12.049

Yu, K., Jacob, D. J., Fisher, J. A., Kim, P. S., Marais, E. A., Miller, C. C., … Wisthaler, A. (2016). Sensitivity to grid resolution in the ability of a chemical transport model to simulate observed oxidant chemistry under high-isoprene conditions. *Atmospheric Chemistry and Physics*, *16*(7), 4369–4378. https://doi.org/10.5194/acp-16-4369-2016